Applied Clay Science 72 (2013) 175–183

Contents lists available at SciVerse ScienceDirect

Applied Clay Science

journal homepage: www.elsevier.com/locate/clay

Research paper

Adsorption of diuron on mechanically and thermally treated montmorillonite and sepiolite

C. Maqueda [a], M. dos Santos Afonso [b,*], E. Morillo [a], R.M. Torres Sánchez [c,**], M. Perez-Sayago [a], T. Undabeytia [a]

[a] Instituto de Recursos Naturales y Agrobiología de Sevilla, (IRNAS-CSIC), Apartado 1052, Sevilla, Spain
[b] INQUIMAE y DQIAQF, Facultad de Ciencias Exactas y Naturales, Universidad de Buenos Aires, Ciudad Universitaria, Pabellón II, C1428EHA, Buenos Aires, Argentina
[c] CETMIC, CC 49, (B1896ZCA) M.B. Gonnet, Provincia de Buenos Aires, Argentina

ARTICLE INFO

Article history:
Received 17 October 2011
Received in revised form 15 October 2012
Accepted 31 October 2012
Available online 20 December 2012

Keywords:
Sepiolite
Montmorillonite
Diuron
Adsorption
Mechanical treatment
Thermal treatment

ABSTRACT

The effects on montmorillonite (Mt) and on sepiolite (Sep) of mechanical (60 and 180 s grinding time) and further thermal treatments (TT) at 500 °C during 24 h, for removing diuron from aqueous solutions were evaluated. The adsorbents and complexes formed were characterised. The specific surface area (SSA), SEM, XRD and zeta potential of the clay mineral samples were determined. The SSA values showed an increase of 50% for ground Mt and a slight decrease for ground Sep. TT reduced SSA by 50% for the Sep samples, but similar values remained for the Mt samples. Both minerals showed a decrease in crystallinity with increasing grinding time and TT. The zeta potential showed an increased of the negative surface charge for the Mt ground samples, but no changes were noticed for the Sep ground samples. The Mt-TT samples showed a slight decrease whilst the Sep samples showed an increase of the negative surface charge in comparison to those without thermal treatment. The adsorption of diuron on Mt was lower than on Sep, and it decreased slightly after 60 and/or 180 s of grinding, despite the larger SSA values. This differences on the adsorption extent were probably due to the increased micropore surface. In contrast, thermal activation caused significantly increased adsorption, especially for the 180-s ground sample that was inversely correlated with the micropore surface, indicating that diuron was not adsorbed in micropores. Diuron adsorption on Sep was higher than on Mt due to its higher SSA. The adsorption capacity of Sep samples was increased by mechanical treatments (ground and sonicated). Moreover, thermal activation led to additional increases in adsorption probably due to changes in the Sep structure by the loss of OH structural groups leading to a more hydrophobic surface. Diuron adsorption on Mt-TT samples produced an increase in the negative surface charge compared to the original sample, whereas a decrease in the negative surface charge was observed for Sep.

1. Introduction

Controlling water pollution is an environmental priority. Monitoring surveys carried out in the United States and Europe have indicated that the use of pesticides in agricultural and non-agricultural media has caused contamination of surface and ground water through runoff and soil leaching (Konstantinous et al., 2006; Yu et al., 2008). The EU has dictated a maximum concentration of 0.1 μg L^{-1} for each pesticide and of 0.5 μg L^{-1} for all pesticides in drinking water (Directive 2000/60/EC).

The herbicide diuron is widely used in agriculture, and its presence in surface and ground water has consequently increased (Claver et al., 2006; Field et al., 2003; Gregorie et al., 2010; Postigo et al., 2010). Adsorption on solid surfaces is an important strategy for controlling the presence of organic contaminants in water. Clay minerals have been proposed as adsorbents to remove hazardous compounds from polluted waters. Clay minerals are natural, abundant and inexpensive materials; they are widely applied in many fields as adsorbents for heavy metals ions (Bradl, 2004), pesticides (Aydin et al., 2009; González-Pradas et al., 2003), dyes (Liu and Zhang, 2007), etc.

Sepiolite (Sep) is a microfibrous hydrated magnesium phyllosilicate with a theoretical unit cell formula of $Si_{12}O_{30}Mg_8(OH,F)_4(OH_2)_4 8H_2O$ formed by blocks and cavities (tunnels) growing in the direction of the fibres. Each structural block is composed of two tetrahedral silica sheets and a central magnesia sheet. Silanol groups (Si–OH) are on the external surface of the silicate particles and are accessible to reagents. The tunnels are filled with water molecules coordinated with the Mg^{2+} ions at the edge of the structure, and zeolitic water is associated by hydrogen bonding to the former. Sep has a high BET specific surface

* Corresponding author. Tel.: +54 11 4576 3380.
** Corresponding author. Tel.: +54 221 484 0247.
E-mail addresses: dosantos@qi.fcen.uba.ar (M. dos Santos Afonso), rosats@cetmic.unlp.edu.ar (R.M. Torres Sánchez).

0169-1317/$ – see front matter © 2012 Elsevier B.V. All rights reserved.
http://dx.doi.org/10.1016/j.clay.2012.10.017

area (SSA), which allows for adsorption of water, polar liquids, ions and molecules such as drugs, insecticides and pesticides (González-Pradas et al., 2005).

Montmorillonite (Mt) presents a layered structure consisting of a sandwich of one octahedral alumina sheet between two tetrahedral silica sheets, with substitutions of some tetrahedral Si atoms by Al atoms and/or of octahedral atoms (Al^{+3} or Mg^{+2}) by atoms with lower oxidation number. The negative charge surface is balanced by exchangeable cations (mainly Na^{+} and Ca^{2+}) located in the interlayer space. Because of its specific properties (high cation exchange capacity (CEC), adsorption, high SSA and swelling), it is widely used for many applications such as environmental remediation.

Mechanical treatments of clay minerals are of great interest because they produce materials with high SSA (Maqueda et al., 2007; Stepkowska et al., 2001; Torres Sánchez et al., 1988) that can be used as adsorbents for different contaminants. Ultrasound has recently been proposed for particle size reduction. Cavitational collapse during the sonication of solids leads to microjet and shock-wave impacts on the surface, together with interparticle size reduction (Pérez-Maqueda et al., 2004a,b). Sonication not only produces a delamination effect but also breaks the layers, whilst the crystalline character is retained (Wiewiora et al., 2003). Sonication of fibrous minerals such as Sep can cause gelling of the dispersions (Simontom et al., 1998). However, studies about the formation and properties of gels prepared from Sep are lacking (Alvarez, 1984; Ovcharenco et al., 1994). Moreover, there are only a few studies about the preparation of Sep gels with pesticides (Maqueda et al., 2008, 2009).

The adsorption capacity of Sep and Mt may be enhanced by thermal modification, which is a commonly used technique for modifying clay minerals (Dekany et al., 1999). Heat treatment of Sep generally reduces the specific surface area, which may be due to narrowing of the intercrystalline channels and loss of OH structural groups (González-Pradas et al., 2005). On the other hand, heating causes micropore plugging due to crystal folding (Balci, 1999), which can increase the adsorption capacity for pesticides. The heating of Mt above 450 °C causes partial destruction of the original structure, small changes in the SSA and movements of the cations within the octahedral sheet (Emmerich, 2000). In addition, calcination modifies the textural properties and dispersibility in water, which can enhance pesticide adsorption (Bojemueller et al., 2001).

The objective of the present research was to evaluate the effectiveness of mechanical and further thermal treatments of Mt and Sep in removing diuron from aqueous solution and to characterise the adsorbents and complexes formed.

2. Materials and methods

2.1. Materials

Montmorillonite from Argentine North Patagonia (Rio Negro) was supplied as raw material by Castiglioni, Pes y Cia. The Mt mineralogy, as evaluated by X-ray diffraction (XRD) and chemical analysis, was previously reported (Viseras Iborra et al., 2006). The Mt sample consists of Na-rich Mt (>84%) with minor phases of quartz and feldspars and with a CEC of 105 meq 100 g^{-1} (Lombardi et al., 2003). The Mt used in this work is a Mt with an interlayer space cations composition of 3.35, 1.08 and 0.26% for Na_2O, CaO and K_2O, respectively (Magnoli et al., 2008). Sep from Vallecas (Madrid, Spain) was supplied by Tolsa, S.A. The mineralogical characterisation of the sample evaluated by XRD showed that the major component was Sep, although calcium carbonate and quartz were also present as minor components (Martínez-Ramírez et al., 1996).

The commercial formulation of the pesticide diuron (3-(3,4-dichlorophenyl)-1,1-dimethylurea, Diurokey, 80%) was supplied by Industrial Quimica Key S.A. (Lerida, Spain). The structural formula of diuron is shown in Fig. 1. Diuron has not acid base properties in the pH range studied thus, the non ionic molecular specie is predominant.

2.2. Sample preparation

The raw samples were ground in a Herzog HS-100 mill for 60 s (Mt60, Sep60) and 180 s (Mt180, Sep180). Other fraction of Sep (1 g) was ultrasonicated for 1 h in 100 mL of distilled water using a Misonix ultrasound liquid processor with a 600 W output, 20 kHz converter and a tapped titanium disruptor horn with a 12.7 mm diameter. The temperature of the reactor was kept constant at 20 °C throughout the entire treatment by recirculating a cooling solution. The obtained clay–gel was lyophilised by placing it in a freezer for 24 h and then freeze-dried with a Virtis Sentry 5 L instrument. The lyophilised material is referred to Sepgel. The Mt was not used as a gel because an emulsion was obtained after the sample sonication and not a real gel.

The Mt and Sep samples ground for 60 and 180 s (Mt60, Sep60, Mt180, Sep180), and the lyophilised sepiolite-gel (Sepgel) were further thermally treated at 500 °C for 24 h (TT). These samples are referred to Mth, Mt60h, Mt180h, Seph, Sep60h, Sep180h and Sepgelh.

2.3. Sample characterisation

Leaching of cations (Al^{+3} and Mg^{+2}) from all of the samples was measured by ICP in a centrifuged solution of a sample dispersion (KCl 10^{-3} and pH 3) after 30 min of contact time.

The isoelectric point (IEP) determinations were performed by measuring the diffusion potential on 80 g L^{-1} (or 8% dispersion) pulp samples with 1 mM KCl as the support electrolyte, as described elsewhere (Torres Sánchez, 1996). Repeated measurements showed pH deviations of ±0.2 units. Zeta potential measurements were performed with a Zeta Plus Zeta Potential Analyzer from Brookhaven Instruments Corporation, using 0.5 g L^{-1} dispersions in 10^{-3} M KCl (inert electrolyte) with HCl or KOH to adjust the dispersion pH.

The SSA was determined in duplicate using the Brunauer Emmet Teller (BET) method. The adsorption of N_2 was measured with a Micromeritics 2200 A (Norcross GA) automatic system (Maqueda et al., 2007). The samples were out-gassed by heating at 200 °C under a flow of helium for 12 h. The data were recorded with p/po between 0.0005 and 0.99. Repeated measurements showed SSA deviations lower than 2%.

The samples with and without diuron adsorbed were studied by XRD on semi-oriented powder samples using CuKα radiation with a Philips PW 1710 diffractometer. The conditions used were a power supply at 40 kV and 30 mA, 1° divergence and detector slits, 0.02° (2θ) step size, counting time of 10 s/step and patterns collected from 3° to 14° (2θ).

Scanning electron microscopy (SEM) was performed on a Zeiss Model Supra40 instrument with a field emission gun. The SEM images were taken by applying a voltage of 5 kV with different magnification times for clarification of the surface. Samples were fixed to 10-mm metal mounts using carbon tape and spit coated with gold under

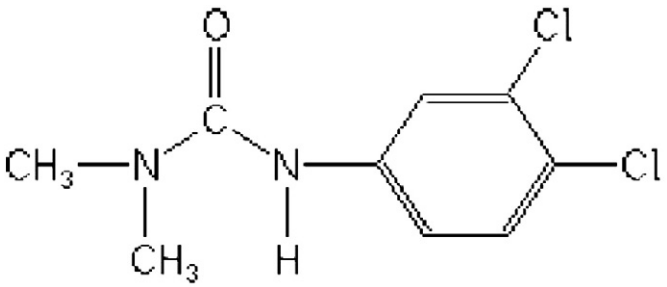

Fig. 1. Structural formula of diuron.

a vacuum in an argon atmosphere. The surface morphology of the coated samples visualised by SEM permitted identification of structural features on the sample surfaces.

2.4. Adsorption of the herbicide

Before conducting the adsorption experiments, preliminary kinetic studies were carried out. Twenty-four hours was found to be long enough to reach pseudo-equilibrium. Triplicate adsorption experiments were performed by mixing 0.2 g of the different samples (raw minerals after grinding at several times and further heated) with a 10 mL solution containing various concentrations (1 to 30 mg L^{-1}) of diuron in 50 mL polypropylene centrifuge tubes. The samples were shaken on a platform shaker for 24 h at 20 ± 1 °C. After shaking, the dispersions were centrifuged, and the concentration of diuron in the supernatant was determined by HPLC. The differences in the initial and final herbicide concentrations were assumed to be due to adsorption.

The adsorption isotherms were fitted to the Freundlich equation:

$$\log Cs = \log K_F + n \log Ce,$$

where Cs (μmol kg^{-1}) is the amount of herbicide adsorbed at the equilibrium concentration Ce (μmol L^{-1}), and K_F and n are constants describing the relative adsorption capacity and the adsorption intensity of the herbicide, respectively.

2.5. Herbicide analysis

HPLC was employed for diuron analysis. The conditions were as follows: mobile phase, acetonitrile:water (60:40); flow, 1 mL min^{-1}; chromatographic column, Kromasil C18 reverse phase; UV detector (Shimadzu 2010 AHT series); wavelength, 230 nm.

3. Results and discussion

3.1. Sample characterisation

Table 1 summarises the IEP_{pH}, SSA, pore volume, pore diameter and micropore values of the mechanically treated and further heated Mt samples.

The SSA values for the ground Mt samples (before and after heating at 500 °C for 24 h) increased by approximately 100% compared to those of Mt and Mth. The SSA value of the Mt sample increased slightly from 47.20 $m^2\ g^{-1}$ to 49.22 $m^2\ g^{-1}$ after heating at 500 °C. Bojemueller et al. (2001) indicated that the SSA value of a Wyoming Greenbond Mt increased from 24.30 $m^2\ g^{-1}$ to 25 $m^2\ g^{-1}$ after heating up to 500 °C for 12 h. However, these authors found striking changes in the SSA values when the calcined samples were dispersed in water.

After the mechanical treatment, the micropore volume increased with increasing grinding time. The average pore diameter decreased after grinding. After heating, the pore diameter of the unground and ground samples increased, whereas the pore volume increased only for the Mt sample, in agreement with Bojemueller et al. (2001). The micropore volume of the heated samples decreased for the ground samples, especially for Mt180h.

The increase in IEP_{pH} with grinding time for the Mt samples was in agreement with the results found for other Mt samples with similar treatments (Torres Sánchez, 1997). The increase was attributed to Al release to the solution, with the consequent enrichment of aluminium ions or hydroxoaluminium species at the edges and at the face (+) and edge (−) contacts (Bojemueller et al., 2001). Further thermal treatment increased the IEP_{pH} to approximately 10 for all of the samples, indicating changes in the hydroxoaluminium species formed (Torres Sánchez et al., 2002). Leaching of the main cations (Al^{+3} and Mg^{+2}) was performed at pH 3 and an ionic strength of KCl 10^{-3} M. The data from the release experiments are shown in Table 2.

The zeta potential curves for the Mt, mechanically treated Mt and TT samples are shown in Fig. 2. The typical flat curve was observed (Fig. 2A) at zeta potential values of approximately −30 mV for the Mt sample (Durán et al., 2000; Lombardi et al., 2006), increasing to approximately −25 mV when the grinding treatment was applied to the Mt60 and Mt180 samples. This change in zeta potential value for the ground samples was attributed to a decrease in the net negative surface charge due to the release of structural Al^{+3} and Mg^{+2} (Table 2), in a similar way as was indicated for the IEP_{pH} increase of these two samples. These effects could lead to the formation of larger aggregates.

The additional thermal treatment (Fig. 2B) generated a similar decrease in the net negative surface charge for Mth with respect to Mt, as was previously found for ground samples and was also attributed to the Al behaviour. The increase of negative surface charge found for the Mt60h and Mt180h samples compared to the Mt60 and Mt180 samples was attributed to changes in the Al coordination sphere after both treatments and are associated with decreased aluminium or magnesium release (Table 2).

The IEP_{pH} values measured by diffusion potential and zeta potential data exhibit apparent inconsistencies, which are originated besides of the used methods, in the structure of clay minerals (Thomas et al., 1999). The original structural charge of smectites is compensated by cations, which are located in the Stern and diffuse layers. The colloids with constant charge would not produce electrokinetic phenomena (zeta potential or electrophoretic measurements, EM) (Thomas et al., 1999). However, when measuring the zeta potential of these minerals as a function of pH, a negative and constant zeta potential value (Fig. 2), which is assigned to the 'basal charge', results from partitioning of the released Al^{+3} or Mg^{+2} cations produced by grinding and/or thermal treatment (Table 2).

The zeta potential variation indicated charge modification of the edge faces, which is consistent with leaching of the different cations and the likely further formation of a mixed cation hydroxide phase

Table 1
IEP, SSA, volume pore, pore diameter and micropore values of Mt samples. Errors are less than 2% and IEP_{pH} deviations are lower than 0.2 pH units.

Sample	IEP_{pH}	SSA $m^2\ g^{-1}$	Pore volume $cm^3\ g^{-1}$	Pore diameter (Å)	Micropore	
					Surface $m^2\ g^{-1}$	Volume $cm^3\ g^{-1}$
Mt	2.7	47.20	0.0647	54.87	15.15	0.0067
Mt60	4.5	101.31	0.0929	36.71	33.40	0.0148
Mt180	5.5	103.75	0.1022	39.43	94.29	0.0448
Mth	6.3	49.22	0.0946	77.47	16.05	0.0073
Mt60h	11.6	88.64	0.0882	39.82	23.44	0.0108
Mt180h	10.4	103.84	0.1005	54.54	26.38	0.0121

Table 2
Aluminium and magnesium release after 30 min contact time, at pH 3 and ionic strength of KCl 10^{-3} M. Errors are less than 2%.

Sample	Al^{+3} mg/L	Mg^{+2} mg/L
Mt	0.144	0.317
Mt60	0.257	0.726
Mt180	0.036	1.248
Mth	0.326	0.381
Mt60h	0.101	0.529
Mt180h	0.049	0.507
Sep	–	1.841
Sep60	–	1.864
Sep180	–	2.544
Seph	–	2.898
Sep60h	–	2.176
Sep180h	–	2.604

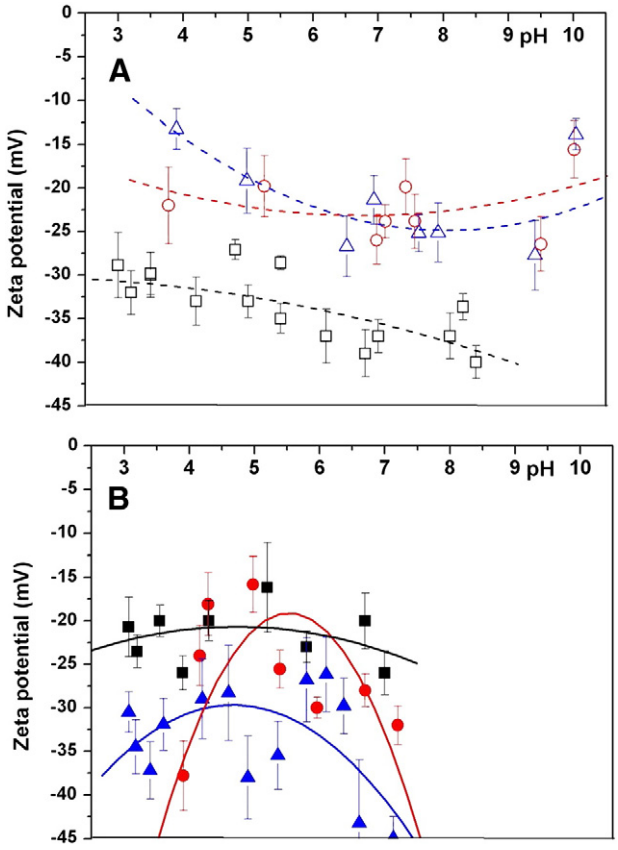

Fig. 2. Zeta potential curves for: (A) empty symbols Mt, and Mt mechanical treated samples and (B) full symbols, for TT samples. Symbols indicate: (■, □) Mt and (●, ○) Mt60 and (▲, △) Mt180. The fitting lines are a linear regression using a polynomial curve. Those lines are located on the graph to assist viewing the curve taking in account the data dispersion.

on the mineral surfaces, depending on the dispersion pH (Scheidegger et al., 1997).

The IEP_{pH}, SSA, pore volume, pore diameter and micropore values of Sep samples are shown in Table 3. Contrary to the results found for Mt samples, the grinding treatment did not increase the SSA values and instead led to decreased values of 10% for Sep180. A short grinding time generated a separation of the Sep fibres. By contrast, a long grinding time produced an amorphous coating on the particles, which decreased the SSA or the cementation of small pores between the crystallites inside the crystalline grains (Cornejo and Hermosin, 1988; Kojdecki et al., 2005; Vucelic et al., 2002). The micropore surface represents about the 50% of the SSA, remaining the values very similar after grinding; therefore, the nano-channels were not destroyed. A decrease of approximately 40% in the SSA values was observed after heating. This behaviour is in agreement with results reported by Balci (1999), indicating that the thermal treatment at temperatures higher than 100 °C led to a decrease in SSA for Sep. The heat treatment produced a decrease in the SSA values, which may be due to narrowing of the intercrystalline channels (Fernández-Álvarez, 1970). After heating at 500 °C, there was a decrease in the non-microporous SSA ($SSA\text{-}S_{micropore}$) and a loss of microporosity of Sep, as suggested by Caturla et al. (1999). The heating produced an important decrease of the micropore surface and volume compared with the unheated sample. Sonication did not decrease the SSA surface (sample Sepgel) because the crystalline character was retained.

Table 3
IEP, SSA, volume pore, pore diameter and micropore values of Sep samples. Errors are less than 2% and IEP_{pH} deviations are lower than 0.2 pH units.

Sample	IEP_{pH}	SSA $m^2\ g^{-1}$	Pore volume $cm^3\ g^{-1}$	Pore diameter (Å)	Micropore	
					Surface $m^2\ g^{-1}$	Volume $cm^3\ g^{-1}$
Sep	7.9	248	0.35	56.80	120.00	0.055
Sep60	8.2	243	0.30	49.98	136.44	0.063
Sep180	8.4	218	0.28	51.26	112.52	0.052
Sepgel	8.0	257	0.40	62. 69	101.78	0.046
Sh	10.4	133	0.40	93.04	28.54	0.012
Sep60h	11.5	162	0.32	78.70	54.90	0.026
Sep180h	10.5	167	0.27	62.83	84.37	0.039
Sepgelh	8.5	145	0.59	154.49	17.33	0.007

The IEP_{pH} value found for the Sep sample was in agreement with the results reported by Alkan et al. (2005), despite differences in methodologies and concentrations used. A slightly increased IEP_{pH} value was found with longer grinding time, increasing more than 2 pH units with further heating (more than pH 10).

The higher IEP_{pH} values obtained for Sep than for the Mt samples were attributed to an acid–base interaction of the Sep surface, which generated a strong buffering capacity in the vicinity of pH 8.5 and Mg^{+2} release from this clay mineral into the solution (Table 2). Similar results were previously found by Kara et al. (2003). The smaller increase in the IEP_{pH} values for Sep than for the Mt samples with the same grinding time was attributed to the increase of $M-O^-$ or $M-(OH)_2^-$ groups due to dehydroxylation or deprotonation of the surface (Alkan et al., 2005).

The zeta potential (figure not shown) for the Sep samples (Sep, Sep60, Sep180, and Sepgel) indicated a negative surface charge over the entire pH range studied, as found for Mt, but no significant differences in the negative surface charge were found for Sep and for all of the ground samples. The shape and pH crosspoint differences in the zeta potential curve of the Sep sample between this study and those reported by Alkan et al. (2005) and Dogan et al. (2009) were attributed to different provenance and sample purity, and isolation of larger particles (Özdemir et al., 2007), which would generate different octahedral Mg^{+2} exchange followed by release into solution and consequent acidification. Small impurities in the Sep sample (Pérez-Rodríguez and Galán, 1994) could result in differences of the zeta potential curve. Further heating generated a slight increase in the net negative surface charge for Sep, contrary to the results found for Mt, and associated to the high amount of Mg^{+2} release (Table 2).

The SEM micrographs of Mt and Sep are shown in Fig. 3. No significant changes were observed in the shape of the particles for the Mt sample, but some agglomeration was found with increasing grinding time due to a reduction in the face-to-edge contacts.

The fibrous nature of Sep was evidenced from the scanning electron micrographs (Fig. 3A). The fibres were arranged in bundles, with lengths of 2–10 μm (Maqueda et al., 2009; Vucelic et al., 2002). After 60 s of grinding (Fig. 3B), the fibre size was reduced to 0.2–0.5 μm. After 180 s of treatment, the particles appeared as irregular spheres, with diameters of up to 20 nm (Fig. 3C). This shape resulted from the impact of the grinding rings and from interparticle collisions, suggesting that the particles were amorphised to an extent.

The XRD patterns are shown in Fig. 4 in a semi-oriented condition for the Mt and Sep samples. The XRD pattern (Fig. 4A) of the Mt sample showed a (001) reflection at 1.23 nm, indicating a water monolayer at the interlayer space (Cases et al., 1997; Magaña et al., 2008). Mechanical treatment led to some amorphisation, as revealed by damage at the *c*-axis (Christidis, et al., 2005) and by diminution and broadening of the (001) reflection. Further thermal treatment (Fig. 4B) produced a shift in (001) reflection to approximately 0.97 nm, corresponding to a thickness of a single Mt layer (Harris et al., 1999).

The Sep samples showed a broadening and diminution of the (110) reflection after mechanical treatment (Fig. 4A), similar to that found for the (001) reflection for the Mt samples. The Sep reflections at 060, 131 and 260, corresponding to 0.46, 0.43 and 0.37 nm, exhibited

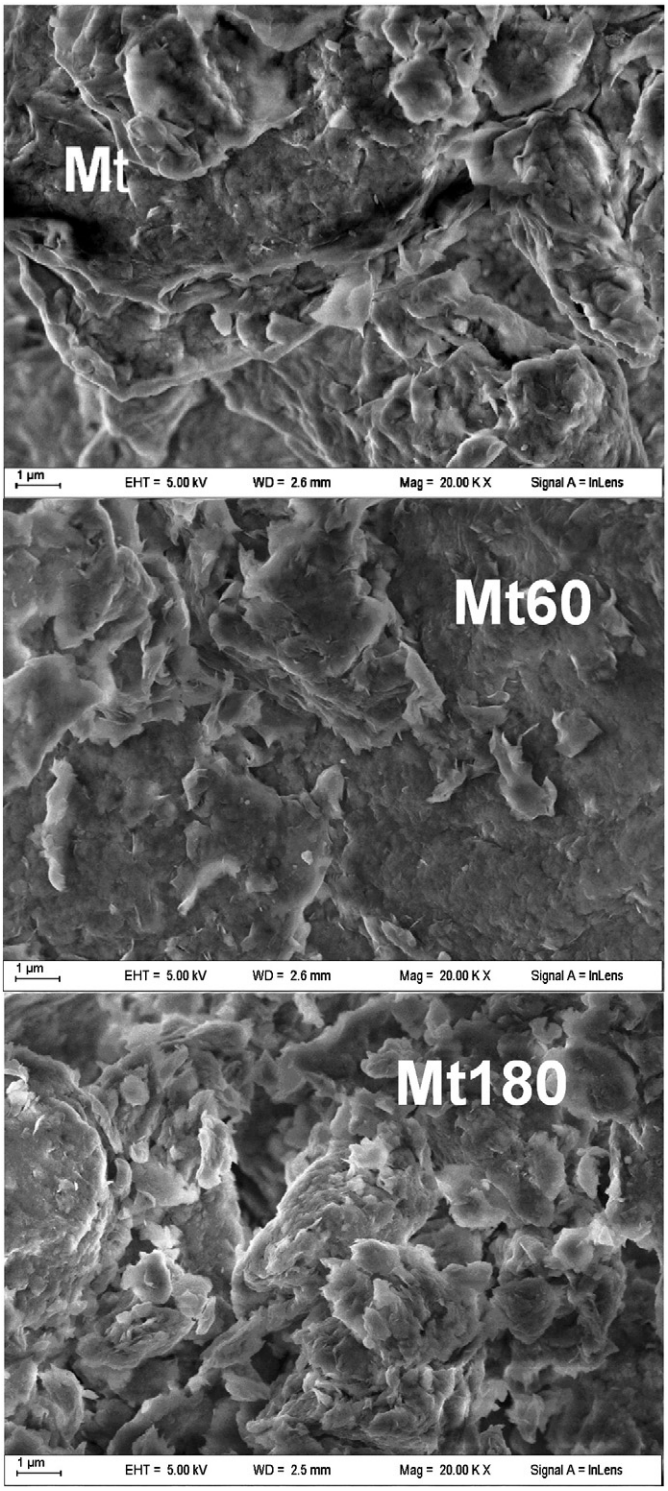

Fig. 3. SEM micrographs of raw and milled products at 60 and 180 s, respectively.

a similar behaviour as the (110) reflection (Kojdecki et al., 2005). Thermal treatment of the Sep and Sepgel samples (Fig. 4B) generated further amorphisation and a shift of the (110) reflection to 0.98 nm and 1.02 nm, respectively, indicating folding of the structure and removal of the hydroxyl groups in the octahedral layers (Mora et al., 2010; Post et al., 2007). The (110) reflection at 1.19 nm was slightly shifted to approximately 1.24 nm for the Sep60h and Sep180h samples, whilst an intermediate value at 1.02 nm was found for the Sepgelh sample.

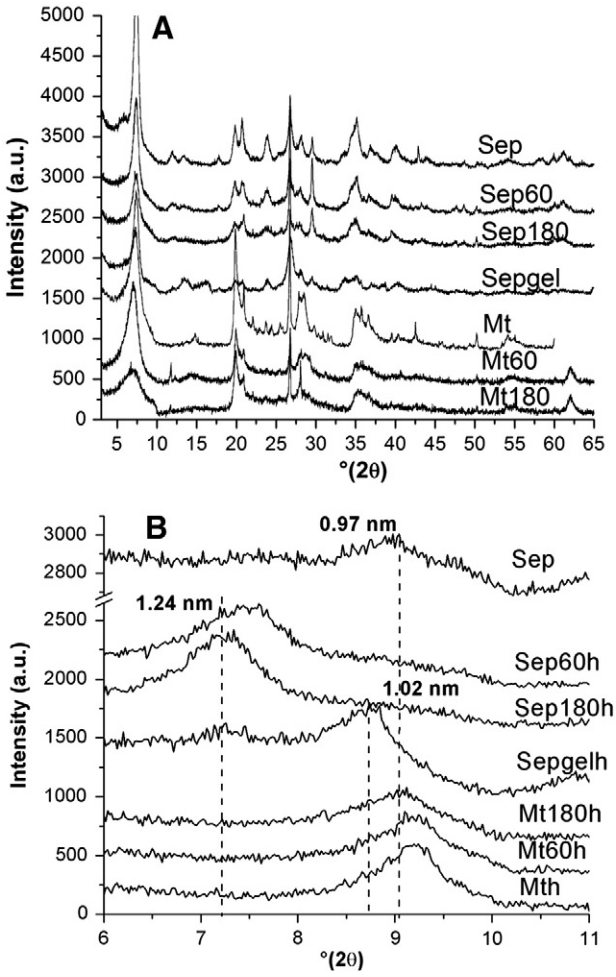

Fig. 4. XRD patterns in semi-oriented condition for: (A) Mt and Sep and their ground samples and (B) partial XRD patterns for TT samples.

In general, the XRD patterns showed a decrease in crystallinity with increasing grinding time and additional thermal treatment, as indicated by a decrease in the intensity of the main reflections.

3.2. Diuron adsorption

3.2.1. Montmorillonite

The adsorption isotherms of diuron on unground and ground Mt and Sep samples are shown in Fig. 5. The small amount of diuron adsorbed on the Mt samples relative to other non-ionic pesticides, such as carbaryl and dichlobenzyl (Sheng et al., 2001) or thyabendazole (Lombardi et al., 2003), decreased slightly after grinding. The low values of diuron adsorption in Mt are in agreement with the values found by other authors (Polati et al., 2006). Mechanical treatment of clay minerals usually generates materials with high SSA, which improves their use as adsorbents of different contaminants. In fact, grinding increased the SSA from 47.20 $m^2\ g^{-1}$ for Mt to 103.75 $m^2\ g^{-1}$ for Mt180 and simultaneously increased the micropore surface. The percentage ratio of the micropore surface to the SSA increased from 32.1% for Mt to 32.9% and 90.9% for Mt60 and Mt180, respectively. The adsorption capacity for diuron was inversely correlated with the percentage of the micropore surface, showing the importance of the pore size in the adsorption of diuron and indicating that diuron is not adsorbed in the micropores.

On the other hand, the adsorbed amount of diuron increased for all of the samples after heating (Fig. 5A, continuous lines). Notably, the sequence of diuron adsorption on the samples was different for

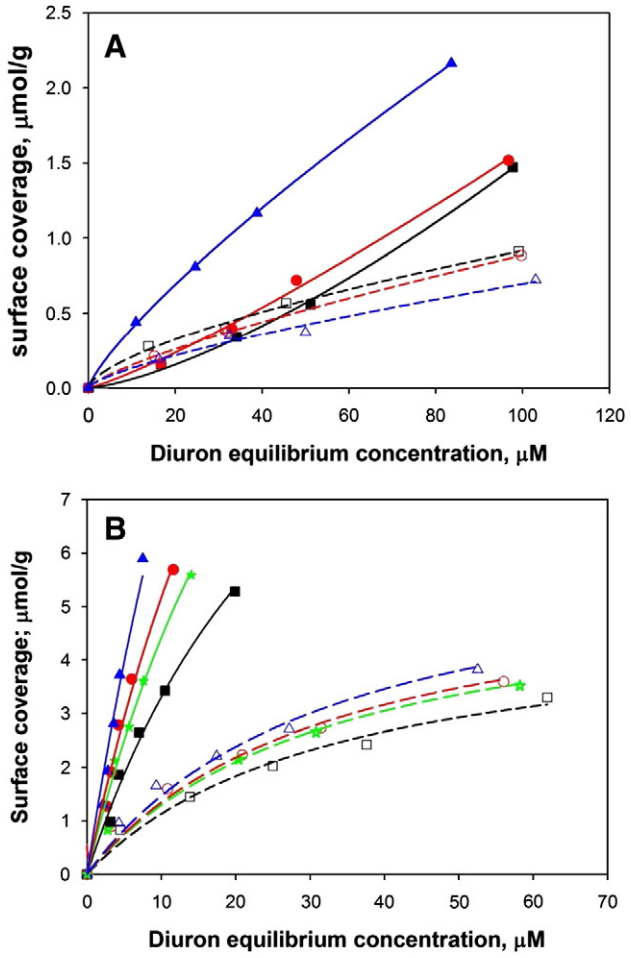

Fig. 5. Adsorption isotherm of diuron on (A) Mt: dotted lines and empty symbols Mt, Mt60, and Mt180 and solid lines and full symbols Mth, Mt60h, and Mt180h, and (B) Sep samples: dotted lines and empty symbols Sep, Sep60, and Sep180, and solid lines and full symbols Seph, Sep60h, and Sep180h. Symbols indicate: (■, □) Mt, (●, ○) Mt60, (▲, △) Mt180, (■, □) Sep, (●, ○) Sep60, (▲, △) Sep180 and (✱, ✳) Sepgel samples.

the unheated and heated samples. The Mt180h sample presented the highest adsorption capacity, whilst the lowest capacity was observed for Mth, in contrast to the results found for the unheated samples. Thermal activation allowed for more than a three-fold increase in adsorption for the Mt180h sample compared to the unheated sample (Mt180). The Mth and Mt60h samples also showed increased adsorption compared with the unheated samples, although in lower proportion than for the Mt180h sample. Thermal treatments of clay minerals remove the intra- and inter-associated water molecules, causing changes in their pore size distribution and consequently in their surface values. The increased adsorption capacity of the heated samples was correlated with the increased SSA values of these samples, contrary to the behaviour of the unheated samples. These results were attributed to the fact that the heated samples generally exhibited a similar SSA value but a smaller micropore surface than their corresponding unheated sample, especially for the Mt180h sample (Table 1). This pattern led to decreased percentages of micropore surface with respect to SSA from 32.6% for Mth to 25.0% for Mt180h, also indicating that diuron is not adsorbed in the micropores.

The experimental adsorption data were fitted to the Freundlich equation (Table 4). The K_F parameter represents the affinity of the sorbent material for the adsorbate, whilst 1/n is related to the surface heterogeneity and the diversity of the energies associated with the adsorption reaction. Because the 1/n values are different among the

Table 4
Freundlich adsorption isotherms parameters of diuron adsorption on the untreated and treated samples, and their respective coefficients of determination (R^2). Errors are less than 2%.

	1/n	K_F*10^3	R^2
Mt	0.65	47.1	0.9956
Mt60	0.76	26.3	1.0000
Mt180	0.72	24.9	0.9848
Mth	1.41	2.3	0.9984
Mt60h	1.18	6.8	0.9964
Mt180h	0.80	63.5	0.9999
Sep	0.54	360	0.9988
Sep60	0.49	500	0.9999
Sep180	0.51	500	0.9979
Sepgel	0.47	520	0.9998
Seph	0.74	590	0.9875
Sep60h	0.84	750	0.9811
Sep180h	1.08	680	0.9895
Sepgelh	0.75	780	0.9991

samples, the K_F values could not be used to determine the adsorption capacities of the different samples. According to the isotherms obtained (Fig. 5A), the order of adsorption was the following: Mt > Mt60 > Mt180. For the heated samples, the order of diuron adsorption was as follows: Mt180h > Mt60h > Mth. The greatly different 1/n values could be indicative of significant heterogeneity among the adsorption surfaces of the samples after the different treatments.

In the heated Mt, most of the adsorption sites are located at the external surface due to the collapse of the layers. The Al ions liberated by the thermal treatment are bound to the external surfaces and edges of the Mt. The enrichment of this species after heating and the textural changes increases the amount of diuron adsorbed. Similar results were observed with adsorption of the herbicide metholachlor on thermally activated Mt (Bojemueller et al., 2001).

The zeta potential curves for the Mt samples after diuron adsorption are shown in Fig. 6. The adsorption of diuron resulted in similar increases in the surface negative charges (to around −45 mV) in mechanically and TT Mt samples in comparison to the same samples without diuron (Fig. 2A and B). Overlapping of the obtained curves (within the error of the method) for all of the samples with adsorbed diuron indicated that a significant surface coating of diuron originated independently of the original particle charge. Planar aromatic structures and electron-withdrawing substituents (e.g., −Cl) seem to favour pesticide adsorption, possibly by formation of an electron donor–acceptor complex between pesticide molecules and siloxane surfaces (Sheng et al., 2001). This electron acceptor surface complex yields a negative charge density on the nitrogen atom that affects the acidity of the adsorbed molecule. Then, the amine proton is more acidic and undergoes very fast deprotonation to yield the corresponding anionic surface complex that increases the surface zeta potential, as shown in Fig. 6. Similar results were found for radical cations obtained during photodegradation of diuron in homogeneous solutions, in which the pK_a shifts from 26 to −0.8 (Canle et al., 2001).

The XRD pattern (figure not shown) of diuron adsorbed on Mt, Mt60 and Mt180 samples showed a shift in the (001) reflection peak of 0.38 nm compared to that of a single Mt layer (0.96 nm, Harris et al., 1999), indicating an increase in the interlayer space. For all samples after thermal treatment, a (001) reflection shift of approximately 0.39 nm was observed.

Based on the spatial position of the N–H and C═O groups, diuron is present in aqueous solutions in two stable geometric conformations classified as trans (Dos Santos et al., 1998). These two trans conformations are planar, and the dimensions of the most stable structure with a relative concentration close to 100% is length = 1.29 nm, width = 0.77 nm and height = 0.74 nm (Fontecha-Cámara et al., 2006). The molecular conformation structure was affected by hydrogen bond formation between diuron and water (Dos Santos

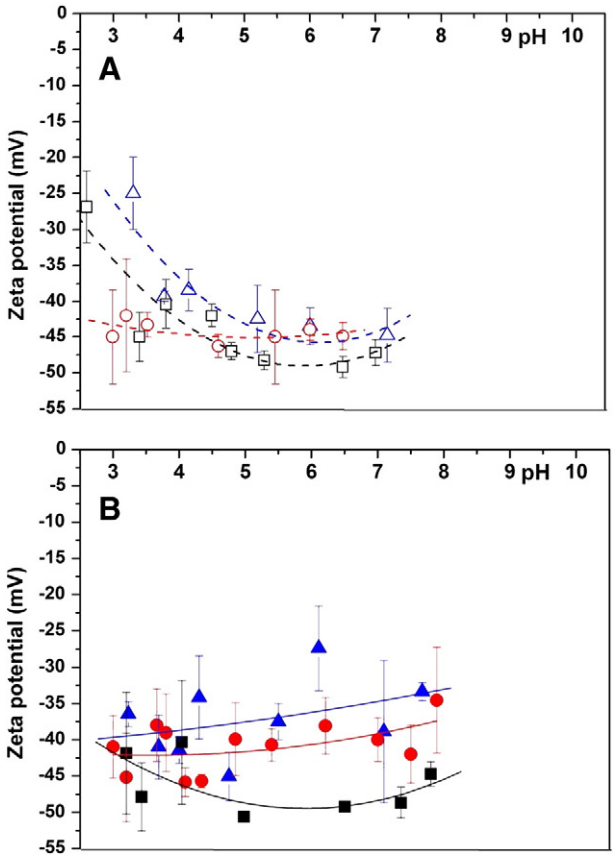

Fig. 6. Zeta potential curves for diuron adsorbed on: (A) empty symbols Mt and Mt mechanical treated samples and (B) full symbols, for, TT samples. Symbols indicate: (■, □) Mt, (●, ○) Mt60 and (▲, △) Mt180. The fitting lines are a linear regression using a polynomial curve. Those lines are located on the graph to assist viewing the curve taking in account the data dispersion.

et al., 1998; Fontecha-Cámara et al., 2006), resulting in a loss of planarity and an increase in height from 0.74 to 1.12 nm. In addition, the dipolar moment of diuron decreased. Thus, the Mt interlayer space increase from 1.23 to 1.35 nm could not be assigned to the entry of diuron molecules (or hydrated diuron molecules) into the interlayer space in a planar configuration, but to water penetration from diuron aqueous solutions, taking into account the extremely low amounts of adsorbed diuron.

3.2.2. Sepiolite

The adsorption isotherms of diuron on the untreated and mechanically treated samples are shown in Fig. 5 (dotted lines). Diuron adsorption on unground Sep was higher than in Mt. Mechanical treatment of Sep increased its adsorption capacity, and thermal activation led to additional increases in adsorption in all samples (Fig. 5, continuous lines). The increase of the slopes of each curve after heating indicates increased affinity of the active sites for diuron.

The experimental data were well fitted to the Freundlich equation. The values of the Freundlich parameters are listed in Table 4. The correlation coefficients were greater than 0.98 in all cases. Because of the similarity of the 1/n values for the unheated and ground samples, the K_F values were compared, showing that the adsorption of diuron was higher for the ground and Sepgel samples than for the unground samples.

The small increase of diuron adsorption on the Sepgel sample compared to Sep was attributed to the increase of the SSA due to the decrease of the packets and the fibre size after sonication and to the decreased micropore surface (Table 3).

In the case of ground Sep, the slightly higher diuron adsorption may be due to modification of the surface heterogeneity produced by grinding, leading to partial amorphisation of the mineral structure.

In spite of the decreased SSA in the thermally activated samples compared to the original Sep and their respective ground samples, diuron adsorption improved. This result was due to changes in the Sep structure owing to the loss of OH structural groups, thereby increasing the relative ratio of siloxane groups on the surface and the OH structural groups. This effect rendered a more hydrophobic surface and allowed the diuron molecules to have more available sites for adsorption on the clay minerals (González-Pradas et al., 2005). This behaviour improved diuron adsorption in spite of the decrease in SSA, most likely also due to a drastic decrease in the micropore surface in comparison to the original Sep sample and their respective ground samples.

Fig. 7 shows the zeta potential curves for diuron adsorbed by the following: (A) Sep and mechanically treated Sep samples and (B) for samples with additional thermal treatment. Diuron adsorption did not change the zeta potential of any of the Sep or mechanically Sep treated samples. A slightly more negative surface charge was observed due to the screening effect of the adsorbed diuron molecules, as observed for the Mt samples. For the TT samples, the diuron adsorption reduced the negative surface charge (approximately 15 mV) of the Sepgelh sample in comparison to the same samples without adsorption (data not shown).

It is well known that the Sep crystals fold by rotation of the fibres on their axes through the Si–O–Si edges bonds that join the fibre units along the lengths of their edges. The folding produces a loss of OH, changing the coordination of the Mg edges. Probably treatment

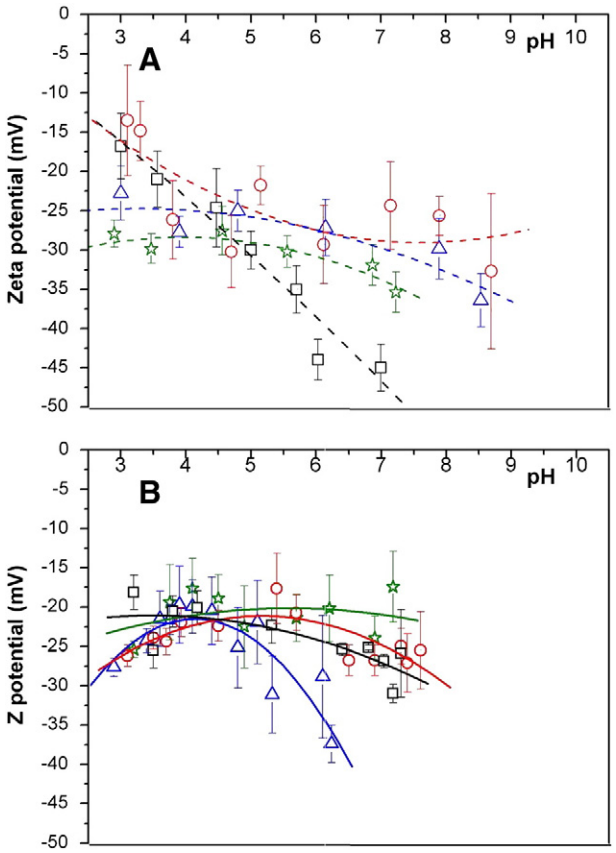

Fig. 7. Zeta potential curves for diuron adsorbed on: (A) empty symbols, Sep and Sep mechanical treated samples and (B) full symbols, for TT samples. Symbols indicate: (■, □) Sep and (●, ○) Sep60, (▲, △) Sep180 and (✱, ✳) Sepgel samples. The fitting lines are a linear regression using a polynomial curve. Those lines are located on the graph to assist viewing the curve taking in account the data dispersion.

with diuron solutions (initial pH of 4.4 and final pH of 8.7) produces some changes of the edges of the octahedral coordination and modifies the zeta potential. Coordination of diuron to the surface likely occurs similarly as for Mt samples, but the change in zeta potential is in the opposite direction (to a less net negative surface charge). In this case, the electron donor–acceptor complex between pesticide molecules and the surface groups locates a positive density charge on the nitrogen atom, leading to a change in the amine nitrogen to a more basic configuration. This behaviour indicates electronic flow in the opposite direction to that observed for diuron adsorbed on Mt most likely due to differences in the electron affinities of magnesium and aluminium (−301 and 50.2 kJ g-ion^{-1}, respectively) in the Sep and Mt structures.

4. Conclusions

The adsorption of diuron on Mt and Sep after mechanical (ground) and thermal treatments was studied. The amount of diuron adsorbed by the Mt samples decreased slightly after grinding, in spite of the larger SSA values, which was due to an increase in the micropore surface. These results indicated that diuron is not adsorbed in the micropores. In contrast, diuron adsorption increased after heating, which was inversely correlated with the micropore surface, also indicating that diuron is not adsorbed on the micropores.

The sequence of diuron adsorption on the heated Mt samples was different from that on the unheated ones. The thermal treatments noticeably decreased the micropore/SSA ratio for the ground samples, improving the herbicide sorption, especially for Mt180h.

The change of the negative charge surface, as shown by the zeta potential curves obtained for all of the samples with increases in the amount of adsorbed diuron, indicated significant coating of the herbicide on the surface.

The adsorption on Sep was four-fold higher than on Mt. Sep modified by mechanical (grinding and sonication) means produced an increase in the diuron adsorption capacity compared with the untreated sample. Additional thermal treatment further increased the adsorption capacity of Sep due to changes in the Sep structure. The micropore surface of the original Sep contributed approximately 50% of the SSA values after grinding because the nano-channels were not destroyed. However, the heat treatment produced a drastic decrease in the micropore surface, on which diuron sorption does not occur.

This study reveals that low-cost clay minerals, especially Sep, can be used to remove diuron from water and could be advantageous over more costly sorbents.

Acknowledgements

The authors acknowledged Buenos Aires University and Collaborative Research and Development Spanish Agency (AECID) for the financial support through A/016047/08 and A/023433/09 grants. Authors are also grateful to Ministerio de Ciencia, Tecnología e Innovación Productiva (MINCyT-Argentina) for financial support through ANPCyT–FONCyT PICT 32678 and 1360 grants. This research was also supported by the MEC project CTM2009-07425 and the Junta de Andalucía Project P09-RNM4581. Both projects received funding from the European Social Fund for financial support.

References

Alkan, M., Tekin, G., Namli, H., 2005. FTIR and zeta potential measurements of sepiolite treated with some organosilanes. Microporous and Mesoporous Materials 84, 75–83.
Alvarez, A., 1984. Sepiolite: properties and uses. In: Singer, A., Galan, E. (Eds.), Palygorskite–sepiolite. Occurrences, Genesis and Uses. Development in Sedimentology, vol. 37. Elsevier, Amsterdam, pp. 253–287.
Aydin, M.E., Ozcan, S., Beluk, F., 2009. Removal of lindane and dieldrin from aqueous solutions by montmorillonite and bentonite and optimization of parameters. Fresenius' Environmental Bulletin 18, 911–916.
Balci, S., 1999. Effect of heating and acid pre-treatment on pore size distribution of sepiolite. Clay Minerals 34, 647–655.
Bojemueller, E., Nennemann, A., Lagaly, G., 2001. Enhanced pesticide adsorption by thermally modified bentonites. Applied Clay Science 18, 277–284.
Bradl, H.B., 2004. Adsorption of heavy metals ions on soil and soil constituents. Journal of Colloid and Interface Science 277, 1–18.
Canle, L.M., Rodríguez, S., Rodríguez Vázquez, L.F., Santaballa, J.A., Steenken, S., 2001. First stages of photodegradation of the urea herbicides Fenuron, Monuron and Diuron. Journal of Molecular Structure 565–566, 133–139.
Cases, J.M., Bérend, I., François, M., Uriot, J.P., Michot, L.J., Thomas, F., 1997. Mechanism of adsorption and desorption of water vapor by homoionic montmorillonite: 3. The Mg^{2+}, Ca^{2+}, Sr^{2+} and Ba^{2+} exchanged forms. Clays and Clay Minerals 45, 8–22.
Caturla, S., Molina-Sabio, M., Rodríguez-Reinoso, F., 1999. Adsorption–desorption of water vapor by natural and heat-treated sepiolite in ambient air. Applied Clay Science 15, 367–380 (1999).
Christidis, G.E., Dellisanti, F., Valdre, G., Makri, P., 2005. Structural modifications of smectites mechanically deformed under controlled conditions. Clay Minerals 40 (4), 511–522.
Claver, A., Omar, P., Rodriguez, L., Ovelleiro, J.L., 2006. Study of the presence of pesticides in surface waters in the Ebro river basin (Spain). Chemosphere 64, 1437–1443.
Cornejo, J., Hermosin, M.C., 1988. Structural alteration of sepiolite by dry gtrinding. Clay Minerals 23, 391–398.
Dekany, I., Turi, L., Fonseca, A., Nagy, J.B., 1999. The structure of acid treated sepiolite: small-angle X-ray scattering and multiMAS-NMR investigations. Applied Clay Science 14, 141–160.
Dogan, M., Turkyilmaz, M., Alkan, M., Demibas, O., 2009. Adsorption of copper (II) ions onto sepiolite and electrokinetic properties. Desalination 238, 257–270.
Dos Santos, H.F., O'Malley, P.J., De Almeida, W.B., 1998. Gas phase and water solution conformational analysis of the herbicide diuron (DCMU): an ab initio study. Theoretical Chemistry Accounts 99, 301–311.
Durán, J.D.G., Ramos-Tejada, M.M., Arroyo, F.J., González-Caballero, F., 2000. Rheological and electrokinetic properties of Na-montmorillonite suspensions. Journal of Colloid and Interface Science 229, 107–117.
Emmerich, K., 2000. Spontaneous rehydroxylation of a dehydroxylated *cis*-vacant montmorillonite. Clays and Clay Minerals 48, 405–408.
Fernández-Álvarez, T., 1970. Superficie específica y estructura de poro de la sepiolita calentada a diferentes temperaturas. In: Serratosa, J.M. (Ed.), Proc. Reunión Hispano Belga de Minerales de la Arcilla. CSIC, Spain, pp. 202–209 (Madrid).
Field, J.A., Reed, R.L., Saweyer, T.E., Griffth, S.M., Wigington, P.J., 2003. Diuron occurrence and distribution in soil and surface and ground water associated with grass see production. Journal of Environmental Quality 32, 171–179.
Fontecha-Cámara, M.A., López-Ramón, M.V., Álvarez-Merino, M.A., Moreno-Castilla, C., 2006. Temperature dependence of herbicide adsorption from aqueous solutions on activated carbon fiber and cloth. Langmuir 22, 9586–9590.
González-Pradas, E., Socias-Viciana, M., Saifi, M., Ureña-Amate, M.D., Flores-Cespedes, F., Fernandez-Perez, M., Villafranca-Sanchez, M., 2003. Adsorption of atrazina from aquous solution on heat treated kerolites. Chemosphere 51, 85–93.
González-Pradas, E., Socias-Viciana, M., Ureña-Amate, M.D., Cantos-Molina, A., Villafranca-Sanchez, M., 2005. Adsorption of chloridazon from aqueous solutions on heat and acid treated sepiolites. Water Research 39, 1849–1857.
Gregorie, C., Payraudeau, S., Domange, N., 2010. Use and fate of 17 pesticides applied on a vineyard catchment. International Journal of Environmental Analytical Chemistry 90, 406–420.
Harris, D.J., Bonagamba, T.J., Schmidt-Rohr, K., 1999. Conformation of poly(ethylene oxide) intercalated in clay and MoS2 studied by two-dimensional double-quantum NMR. Macromolecules 32, 6718–6724.
Kara, M., Yuzer, H., Sabah, E., Celik, M.S., 2003. Adsorption of cobalt from aqueous solution onto sepiolite. Water Research 37, 224–232.
Kojdecki, M.A., Bastida, J., Pardo, P., Amorós, P., 2005. Crystalline microstructure of sepiolite influenced by grinding. Journal of Applied Crystallography 38, 888–899.
Konstantinous, I., Hela, D., Albanis, T., 2006. The status of pesticide pollution in surface waters (rivers and lakes) of Greece. Part I. Review on occurrence and levels. Environmental Pollution 141, 555–570.
Liu, P., Zhang, L.X., 2007. Adsorption of dyes from aqueous solutions of suspension with clay nano-adsorbents. Separation and Purification Technology 58, 32–39.
Lombardi, B., Baschini, M., Torres Sánchez, R.M., 2003. Parameters optimisation and adsorption mechanism of thiabendazole fungicide on Argentine North Patagonia's montmorillonite. Applied Clay Science 24, 43–50.
Lombardi, B., Torres Sánchez, R.M., Eloy, P., Genet, M., 2006. Interaction of thiabendazole and benzimidazole with montmorillonite. Applied Clay Science 33, 59–65.
Magaña, S.M., Quintana, P., Aguilar, D.H., Toledo, J.A., Angeles-Chavez, C., Cortes, M.A., Leon, L., Freile-Pelegrin, Y., Lopez, T., Torres Sánchez, R.M., 2008. Antibacterial activity of montmorillonites modified with silver. Journal of Molecular Catalysis A: Chemical 281, 192–199.
Magnoli, A.P., Tallone, L., Rosa, C.A.R., Dalcero, A.M., Chiacchiera, S.M., Torres Sánchez, R.M., 2008. Commercial bentonites as detoxifier of broiler feed contaminated with aflatoxin. Applied Clay Science 40, 63–71.
Maqueda, C., Romero, A.S., Morillo, E., Perez-Rodriguez, J.L., 2007. Effect of grinding on the preparation of porous materials by acid-leached vermiculite. Journal of Physics and Chemistry of Solids 68, 1220–1224.
Maqueda, C., Villaverde, J., Sopeña, F., Undabeytia, T., Morillo, E., 2008. A novel system for reducing leachng of the herbicide metribizin using clay-gel based formulations. Journal of Agricultural and Food Chemistry 56, 11941–11946.

Maqueda, C., Partal, P., Villaverde, J., Perez-Rodriguez, J.L., 2009. Characterization of sepiolite-gel-based formulations for controlled release of pesticidas. Applied Clay Science 46, 289–295.

Martínez-Ramírez, S., Puertas, S., Blanco-Varela, M.T., 1996. Stability of sepiolite in neutral and alkaline media at room temperatura. Clay Minerals 31, 225–232.

Mora, M., López, M.I., Carmona, M.A., Jiménez-Sanchidrián, C., Ruiz, J.R., 2010. Study of the thermal decomposition of a sepiolite by mid- and near-infrared spectroscopies. Polyhedron 29, 3046–3051.

Ovcharenco, F.D., Kobovki, E.G., Nichiporenco, S.P., Vdovenko, N.V., Tretinnik, V., Kuglitskii, N.N., Panasevich, A.A., 1994. In: Occhavenko, F.D. (Ed.), The Colloid Chemistry of Palygorskite. Israel Program for Scientific Translation, Jerusalem.

Özdemir, O., Çınar, M., Sabah, E., Arslan, F., Sabri, M., Çelik, M.S., 2007. Adsorption of anionic surfactants onto sepiolite. Journal of Hazardous Materials 147, 625–632.

Pérez-Maqueda, L.A., Blanes, J.M., Pascual, J., Pérez-Rodríguez, J.L., 2004a. The influence of sonication on the thermal behaviour of muscovite and biotite. Journal of the European Ceramic Society 24, 2793–2801.

Pérez-Maqueda, L.A., Jiménez de Haro, M.C., Poyato, J., Pérez-Rodríguez, J.L., 2004b. Comparative study of ground and sonicated vermiculite. Journal of Materials Science 39, 5347–5351.

Pérez-Rodríguez, J.L., Galán, E., 1994. Determination of impury in sepiolite by termal analysis. Journal of Thermal Analysis 42, 131–141.

Polati, S., Angioni, S., Gianotti, V., Gosetti, F., Gennaro, M.C., 2006. Sorption of pesticides on kaolinite and montmorillonite as a function of hydrophilicity. Journal of Environmental Science and Health. Part. B 41, 333–344.

Post, J.E., Bish, D.L., Heaney, P.J., 2007. Synchrotron powder X-ray diffraction study of the structure and dehydration, behavior of sepiolite. American Mineralogist 92, 91–97.

Postigo, C., Lopez de Alda, M.J., Barceló, D., Ginebreda, A., Garrido, T., Fraile, J., 2010. Analysis and occurrence of selected medium to highly polar pesticides in groundwater of Catalonia (NE Spain): an approach based on-line solid phase extraction-liquid chromatography-electrospray-tandem mass spectrometry detection. Journal of Hydrology 383, 83–92.

Scheidegger, A.M., Lamble, G.M., Sparks, D.L., 1997. Spectroscopic evidence for the formation of mixed-cation hydroxide phases upon metal sorption on clays and aluminum oxides. Journal of Colloid and Interface Science 186, 118–128.

Sheng, G., Johnston, C.T., Teppen, B.J., Boyd, S.A., 2001. Potential contributions of smectite clays and organic matter to pesticide retention in soils. Journal of Agricultural and Food Chemistry 49, 2899–2907.

Simontom, T.C., Komarneni, S., Roy, R., 1998. Gelling properties of sepiolite versus montmorillonite. Applied Clay Science 3, 165–176.

Stepkowska, E., Perez-Rodriguez, J.L., Jimenez de Haro, M.C., Sanchez-Soto, P.J., Maqueda, C., 2001. Effect of grinding and water vapour on particle size of kaolinite and pyrophyllite. Clay Minerals 36, 105–114.

Thomas, F., Michot, L.J., Vantelon, D., Montarges, E., Prelot, B., Cruchaudet, M., Delon, J.F., 1999. Layer charge and electrophoretic mobility of smectites. Colloids and Surfaces A 159, 351–358.

Torres Sánchez, R.M., 1996. Phase transformations of α to γ-Fe_2O_3 by grinding. Journal of Materials Science Letters 15, 461–462.

Torres Sánchez, R.M., 1997. Mechanochemical effects on physicochemical parameters of homoionic smectite. Colloids and Surfaces A 127, 135–140.

Torres Sánchez, R.M., Aglietti, E.F., Porto Lopez, J.M., 1988. PZC modification on mechanochemically treated kaolinite. Journal of Materials Chemistry and Physics 20 (1), 27–38.

Torres Sánchez, R.M., Boix, A., Mercader, R.C., 2002. Grinding assistance in the transformation of gibbsite to corundum. Journal of Materials Research 17, 712–717.

Viseras Iborra, C., Cultrone, G., Cerezo, P., Aguzzi, C., Baschini, M., Vallés, J., López-Galindo, A., 2006. Characterisation of northern Patagonian bentonites for pharmaceutical uses. Applied Clay Science 31, 272–281.

Vucelic, D., Simic, D., Kovacevic, O., Dojinovic, M., Mitrovic, M., 2002. The effects of grinding on the physicochemical characteristics of white sepiolite from Golesh. Journal of the Serbian Chemical Society 67, 197–211.

Wiewiora, A., Pérez-Rodríguez, J.L., Pérez-Maqueda, L.A., Drapala, J., 2003. Particle size distribution in sonicates high- and low-charge vermiculites. Applied Clay Science 24, 51–58.

Yu, K.W., DeLaune, R.D., Tao, R., Beine, R.L., 2008. Nonpoint sources of nutrients and pesticides associated contamination with sugar cane production and its impact on Louisiana costal water quality. Journal of Environmental Quality 37, 2275–2283.